Available online at www.sciencedirect.com

ScienceDirect

Procedia Computer Science 108C (2017) 1903–1912

Procedia Computer Science

International Conference on Computational Science, ICCS 2017, 12-14 June 2017, Zurich, Switzerland

The THex Algorithm and a Simple Darcy Solver on Hexahedral Meshes

Graham Harper[1] *, Jiangguo Liu[2] †, and Bin Zheng[3]

[1] Department of Mathematics, Colorado State University, Fort Collins, CO 80523-1874, USA, harper@math.colostate.edu

[2] Department of Mathematics, Colorado State University, Fort Collins, CO 80523-1874, USA, liu@math.colostate.edu

[3] Pacific Northwest National Laboratory, P.O.Box 999, Richland, WA 99352, USA, Bin.Zheng@pnnl.gov

Abstract

In this paper, we first present the THex algorithm that refines a tetrahedral mesh into a hexahedral mesh. Strategies for efficient implementation of the THex algorithm are discussed. Then we present the lowest order weak Galerkin (WG) $(Q_0, Q_0; RT_{[0]})$ finite element method for solving the Darcy equation on general hexahedral meshes. This simple solver uses constant pressure unknowns inside hexahedra and on faces but specifies the discrete weak gradients of these basis functions in local Raviart-Thomas $RT_{[0]}$ spaces. Implementation of this solver is straightforward. The solver is locally mass-conservative, and produces continuous normal fluxes, regardless of hexahedral mesh quality. When the mesh is asymptotically parallelopiped, this Darcy solver exhibits optimal order convergence in pressure, velocity, and flux, as demonstrated by numerical results.

Peer-review under responsibility of the scientific committee of the International Conference on Computational Science

Keywords: Darcy equation, hexahedral meshes, lowest order elements, THex algorithm, weak Galerkin

1 Introduction

Darcy solvers have fundamental importance in numerical simulations of flow and transport in porous media. Local mass conservation and normal flux continuity are two important properties desired for Darcy solvers, in addition to stability, optimal order convergence, and easy implementation [4, 10, 12]. Solving the Darcy equation in complicated 3-dim domains could be challenging. Although tetrahedral meshes are fundamentally important, hexahedral meshes are preferred in certain cases, since they require less degrees of freedom (DOFs) but can still accommodate complicated domain geometry.

*This author was partially supported by US National Science Foundation under grant DMS-1419077.

†This author was partially supported by US National Science Foundation under grant DMS-1419077.

1877-0509 © 2017 The Authors. Published by Elsevier B.V.

Peer-review under responsibility of the scientific committee of the International Conference on Computational Science

10.1016/j.procs.2017.05.148

Hexahedral meshes can be generated using commercial softwares, e.g., `Trelis/CUBIT` [1]. A sophisticated algorithm for generating hexahedral meshes is provided in [8]. In a simple way, one could use the freely available software `TetGen` [9] to generate a tetrahedral mesh and then use the THex algorithm to refine the tetrahedral mesh into a hexahedral mesh.

Hexahedral meshes may have nonflat faces that raise challenges to finite element methods for maintaining flux continuity. For the mixed finite element methods, normal flux continuity is obtained by employing the Piola transformation to construct finite element spaces [2, 3, 12]. The weak Galerkin methods [4, 5, 7, 11] adopt a different approach. Pressure basis functions are set inside elements and on edges/faces between elements, but their discrete weak gradients are specified in certain known spaces that have adequate approximation capacity and hence can be used to approximate the classical gradient in the variational form for the Darcy equation. Normal continuity of numerical fluxes is derived from the properties of discrete weak gradients.

Specifically in this paper, we present the lowest order WG finite element method $(Q_0, Q_0; RT_{[0]})$ that uses constant pressure unknowns inside hexahedra and on faces but specifies their discrete weak gradients in local Raviart-Thomas $RT_{[0]}$ spaces. This Darcy solver has easy implementation, is locally mass-conservative, and produces continuous normal fluxes. When the mesh is asymptotically parallelopiped, the method exhibits optimal order convergence in pressure, velocity, and flux, as demonstrated by numerical results.

2 The THex Algorithm

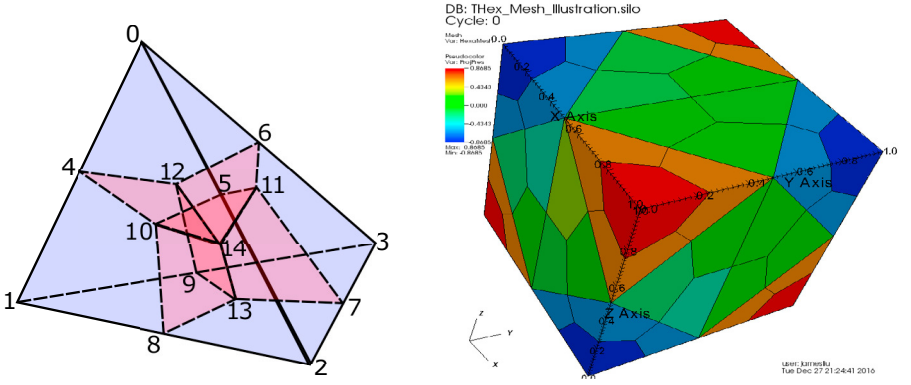

(a) (b)

Figure 1: (a) A tetrahedron partitioned into 4 hexa.; (b) A tetrahedral mesh refined into a hexahedral mesh.

The **THex** algorithm divides each tetrahedron into four (4) hexahedra and hence refines a tetrahedral mesh into a hexahedral mesh. In this process, we see proliferation of nodes, faces, and elements. Besides the original nodes of the tetrahedral mesh, we create (see Fig.1(a))

- A new node at the centroid of each original tetrahedron: Node #14;
- A new node at the centroid of each original triangular face: Node #10,11,12,13;
- A new node at the midpoint of each original edge: Node #4,5,6,7,8,9.

Similarly,

- Each original triangular face is divided into three (3) **flat** quadrilateral faces,
- Six (6) new quadrilateral faces are created inside each original tetrahedron. These new quadrilateral faces are flat also.

See Figure 1 for an illustration of one tetrahedron being partitioned into 4 hexahedra.

For a given tetrahedral mesh, we use respectively `NumNdsT`, `NumEgsT`, `NumFcsT`, `NumEmsT` to denote the numbers of nodes, edges, triangular faces, and tetrahedra. Similarly, we use `NumNdsH`, `NumFcsH`, `NumEmsH` to denote the numbers of nodes, quadrilateral faces, and hexahedra of the resulting hexahedral mesh. Then it is easy to see that

```
NumNdsH = NumNdsT + NumEgsT + NumFcsT + NumEmsT;
NumFcsH = 3*NumFcsT + 6*NumEmsT;
NumEmsH = 4*NumEmsT;
```

It is not difficult to handle just one tetrahedron. However, it is nontrivial to handle an entire tetrahedral mesh. The main difficulty lies in coordinating the orientations of faces and hexahedra.

Suppose the four vertices of a given tetrahedron are labelled locally as $0, 1, 2, 3$ with 0 **being the top (zenith) and** 123 **as the base**, see Figure 1. For the THex algorithm to work correctly, we need to ensure a tetrahedron has the correct orientation by checking its volume being positive and swapping two base vertices if needed.

Clearly, the four triangular faces of the original tetrahedron are

$$\#0 : (0, 1, 2), \quad \#1 : (0, 2, 3), \quad \#2 : (0, 3, 1), \quad \#3 : (3, 2, 1).$$

Note that **the orientation of the base** 123 **(actually now oriented as 321) is somehow different than the other three faces.** This assures that the normal vector points outwards as we traverse the vertices in the given order.

The edges along with their connecting nodes are

$$\#0 : (0, 1), \quad \#1 : (0, 2), \quad \#2 : (0, 3), \quad \#3 : (3, 2), \quad \#4 : (2, 1), \quad \#5 : (1, 3).$$

Accordingly, the midpoints on these edges are labelled as $4, 5, 6, 7, 8, 9$. The centroids of the four faces are labelled as $10, 11, 12, 13$. Finally, the centroid of the tetrahedron is labelled as 14. So the partition scheme uses totally 15 nodes for four hexahedra, whereas the original tetrahedron has only four (4) nodes.

As shown in Figure 1, the new hexahedra have nodal info organized as (on bottom faces and top faces, oriented counterclockwise)

$$\begin{aligned}
\#0 &: (0, 4, 12, 6, \ \ 5, 10, 14, 11) \\
\#1 &: (1, 8, 13, 9, \ \ 4, 10, 14, 12) \\
\#2 &: (2, 7, 13, 8, \ \ 5, 11, 14, 10) \\
\#3 &: (3, 6, 12, 9, \ \ 7, 11, 14, 13)
\end{aligned}$$

It is interesting to see that each new hexahedron involves

- one original node;
- three (adjacent) edge midpoints;

- three face centroids;
- one (the) element centroid.

Note that each of the original four (4) triangular faces of the tetrahedron is partitioned into three (3) quadrilaterals. There are totally twelve (12) such quadrilaterals and they are all **flat**. These 12 flat quadrilateral faces can be expressed as

```
#0: (0,4,10,5),     #1: (1,8,10,4),    #2: (2,5,10,8),
#3: (0,5,11,6),     #4: (2,7,11,5),    #5: (3,6,11,7),
#6: (0,6,12,4),     #7: (3,9,12,6),    #8: (1,4,12,9),
#9: (3,7,13,9),    #10: (2,8,13,7),   #11: (1,9,13,8).
```

In this partition process, six (6) new quadrilateral faces are created inside the original tetrahedron, as shown below

```
#12: (4,10,14,12),   #13: (5,11,14,10),    #14: (6,12,14,11),
#15: (7,13,14,11),   #16: (8,13,14,10),    #17: (9,13,14,12).
```

Each of them appears twice (is shared by two new hexahedra). So there are totally (4*3+6*2) 24 faces. Of course, this is correct, $4 * 6 = 24$.

An important and challenging part of the THex algorithm is to generate the mesh info on elements versus their faces, which is needed by the weak Galerkin, discontinuous Galerkin, and mixed finite element methods. Note that in the THex algorithm, each triangular face of a given tetrahedral mesh is partitioned into four quadrilateral faces, which are faces of the hexahedra resulted from partitioning tetrahedra in the tetrahedral mesh. The global and local orientations of these quadrilateral faces need to be sorted out and coordinated. This can be accomplished using the `set` class in C++ standard template library.

3 A Weak Galerkin Solver for Darcy on Hexahedra

In this section, we present a simple solver for the Darcy equation on hexahedral meshes. This is a novel weak Galerkin method that uses the lowest order elements $(Q_0, Q_0; RT_{[0]})$ on hexahedra. The method is easy to implement but still produces satisfactory results. This approach does not use the Piola transformation. The continuity in normal fluxes is not built in the finite element space but attained through the bilinear form in the numerical scheme.

3.1 WG $(Q_0, Q_0; RT_{[0]})$ Elements for Hexahedra

Let E be a hexahedron with center (x_c, y_c, z_c) and $X = x - x_c, Y = y - y_c, Z = z - z_c$. Let

$$\mathbf{w}_1 = \begin{bmatrix} 1 \\ 0 \\ 0 \end{bmatrix}, \mathbf{w}_2 = \begin{bmatrix} 0 \\ 1 \\ 0 \end{bmatrix}, \mathbf{w}_3 = \begin{bmatrix} 0 \\ 0 \\ 1 \end{bmatrix}, \mathbf{w}_4 = \begin{bmatrix} X \\ 0 \\ 0 \end{bmatrix}, \mathbf{w}_5 = \begin{bmatrix} 0 \\ Y \\ 0 \end{bmatrix}, \mathbf{w}_6 = \begin{bmatrix} 0 \\ 0 \\ Z \end{bmatrix}.$$

We define a local Raviart-Thomas space as

$$RT_{[0]}(E) = \text{Span}(\mathbf{w}_1, \mathbf{w}_2, \mathbf{w}_3, \mathbf{w}_4, \mathbf{w}_5, \mathbf{w}_6). \tag{1}$$

The Gram matrix of the above basis is a 6×6 symmetric positive-definite (SPD) matrix.

We consider 7 discrete weak functions $\phi_i (0 \leq i \leq 6)$ on a hexahedral element E as follows:

- ϕ_0 for element interior: It takes value 1 in the interior E° but 0 on the boundary E^∂;
- $\phi_i (1 \le i \le 6)$ for the six faces respectively: Each takes value 1 on the very face but 0 on all other five faces and in the interior.

Any such a function $\phi = \{\phi^\circ, \phi^\partial\}$ has two independent parts: ϕ° is defined in E°, whereas ϕ^∂ is defined on E^∂. Then its discrete weak gradient $\nabla_{w,d}\phi$ is specified in $RT_{[0]}(E)$ via integration by parts [11] (implementationwise solving a size-6 SPD linear system):

$$\int_E (\nabla_{w,d}\phi)\cdot\mathbf{w} = \int_{E^\partial} \phi^\partial(\mathbf{w}\cdot\mathbf{n}) - \int_{E^\circ} \phi^\circ(\nabla\cdot\mathbf{w}), \quad \forall \mathbf{w} \in RT_{[0]}(E). \tag{2}$$

Specifically, when E becomes a brick $[x_0, x_1]\times[y_0, y_1]\times[z_0, z_1]$, we have

$$\begin{cases}
\nabla_{w,d}\phi_0 = & 0\mathbf{w}_1 + & 0\mathbf{w}_2 + & 0\mathbf{w}_3 + & \frac{-12}{(x_1-x_0)^2}\mathbf{w}_4 + & \frac{-12}{(y_1-y_0)^2}\mathbf{w}_5 + & \frac{-12}{(z_1-z_0)^2}\mathbf{w}_6,\\
\nabla_{w,d}\phi_1 = & \frac{-1}{x_1-x_0}\mathbf{w}_1 + & 0\mathbf{w}_2 + & 0\mathbf{w}_3 + & \frac{6}{(x_1-x_0)^2}\mathbf{w}_4 + & 0\mathbf{w}_5 + & 0\mathbf{w}_6,\\
\nabla_{w,d}\phi_2 = & \frac{1}{x_1-x_0}\mathbf{w}_1 + & 0\mathbf{w}_2 + & 0\mathbf{w}_3 + & \frac{6}{(x_1-x_0)^2}\mathbf{w}_4 + & 0\mathbf{w}_5 + & 0\mathbf{w}_6,\\
\nabla_{w,d}\phi_3 = & 0\mathbf{w}_1 + & \frac{-1}{y_1-y_0}\mathbf{w}_2 + & 0\mathbf{w}_3 + & 0\mathbf{w}_4 + & \frac{6}{(y_1-y_0)^2}\mathbf{w}_5 + & 0\mathbf{w}_6,\\
\nabla_{w,d}\phi_4 = & 0\mathbf{w}_1 + & \frac{1}{y_1-y_0}\mathbf{w}_2 + & 0\mathbf{w}_3 + & 0\mathbf{w}_4 + & \frac{6}{(y_1-y_0)^2}\mathbf{w}_5 + & 0\mathbf{w}_6,\\
\nabla_{w,d}\phi_5 = & 0\mathbf{w}_1 + & 0\mathbf{w}_2 + & \frac{-1}{z_1-z_0}\mathbf{w}_3 + & 0\mathbf{w}_4 + & 0\mathbf{w}_5 + & \frac{6}{(z_1-z_0)^2}\mathbf{w}_6,\\
\nabla_{w,d}\phi_6 = & 0\mathbf{w}_1 + & 0\mathbf{w}_2 + & \frac{1}{z_1-z_0}\mathbf{w}_3 + & 0\mathbf{w}_4 + & 0\mathbf{w}_5 + & \frac{6}{(z_1-z_0)^2}\mathbf{w}_6.
\end{cases}$$

3.2 WG $(Q_0, Q_0; RT_{[0]})$ Finite Element Scheme for Darcy on Hexahedra

In this subsection, we use the previously discussed WG $(Q_0, Q_0; RT_{[0]})$ finite elements on hexahedra to develop a finite element scheme for solving the Darcy equation in its usual form

$$\begin{cases}
\nabla\cdot(-\mathbf{K}\nabla p) \equiv \nabla\cdot\mathbf{u} = f, & \mathbf{x}\in\Omega,\\
p = p_D, & \mathbf{x}\in\Gamma^D,\\
\mathbf{u}\cdot\mathbf{n} = u_N, & \mathbf{x}\in\Gamma^N,
\end{cases} \tag{3}$$

where $\Omega \subset \mathbb{R}^3$ is a bounded polyhedral domain, p the unknown pressure, $\mathbf{K}$ a permeability tensor that is uniformly SPD, f a source term, p_D, u_N respectively Dirichlet and Neumann boundary data, $\mathbf{n}$ the outward unit normal vector on $\partial\Omega =: \Gamma$, which has a nonoverlapping decomposition into the Dirichlet boundary Γ^D and the Neumann boundary Γ^N.

Let $\mathcal{E}_h$ be a quasi-uniform hexahedral mesh for Ω and Γ_h be the set of all faces in the mesh. Accordingly Γ_h^D, Γ_h^N denote the faces on Γ^D and Γ^N, respectively. Let S_h be the space of global discrete weak functions on $\mathcal{E}_h$ that are piecewise constants (degree 0 polynomials) in the element interiors and also piecewise constants (degree 0 polynomials) on the faces. Let S_h^0 be a subspace of S_h consisting of the shape functions that vanish on Γ_h^D.

Seek $p_h = \{p_h^\circ, p_h^\partial\} \in S_h$ (p_h° for the values in all element interiors, p_h^∂ for the values on all faces) such that $p_h^\partial|_{\Gamma_h^D} = Q_h^\partial(p_D)$ (the L^2-projection of the Dirichlet boundary data into the space of all piecewise constant functions on Γ_h^D) and

$$\mathcal{A}_h(p_h, q) = \mathcal{F}(q), \qquad \forall q = \{q^\circ, q^\partial\} \in S_h^0, \tag{4}$$

where

$$\mathcal{A}_h(p_h, q) := \sum_{E\in\mathcal{E}_h} \int_E \mathbf{K}\nabla_{w,d}p_h\cdot\nabla_{w,d}q, \tag{5}$$

and

$$\mathcal{F}(q) := \sum_{E\in\mathcal{E}_h}\int_E fq^\circ - \sum_{\gamma\in\Gamma_h^N}\int_\gamma u_N q^\partial. \tag{6}$$

This results in a symmetric positive-definite sparse linear system, which can be solved using conjugate-gradient type linear solvers.

After the numerical pressure p_h is solved, a **numerical velocity** $\mathbf{u}_h$ is obtained elementwise via a local L_2-projection $\mathbf{Q}_h$ back into the subspace $RT_{[0]}(E)$:

$$\mathbf{u}_h = \mathbf{Q}_h(-\mathbf{K}\nabla_{w,d}p_h). \tag{7}$$

But the projection can be omitted when $\mathbf{K}$ is an elementwise constant scalar matrix.

Theorem 1 (Local mass conservation). For any hexahedron $E \in \mathcal{E}_h$, there holds

$$\int_E f = \int_{E^\partial} \mathbf{u}_h\cdot\mathbf{n}. \tag{8}$$

Proof. In Equation (4), we take a test function q such that q has value 1 in E° but vanishes everywhere else (in the interiors of all other elements and on all faces). We thus have

$$\begin{aligned}\int_E f &= \int_E (\mathbf{K}\nabla_{w,d}p_h)\cdot\nabla_{w,d}q = \int_E \mathbf{Q}_h(\mathbf{K}\nabla_{w,d}p_h)\cdot\nabla_{w,d}q = \int_E(-\mathbf{u}_h)\cdot\nabla_{w,d}q\\ &= -\int_{E^\partial} q^\partial(\mathbf{u}_h\cdot\mathbf{n}) + \int_E q^\circ(\nabla\cdot\mathbf{u}_h) = \int_E \nabla\cdot\mathbf{u}_h = \int_{E^\partial}\mathbf{u}_h\cdot\mathbf{n},\end{aligned}$$

where we have used the definition of projection $\mathbf{Q}_h$, the definite of discrete weak gradient, and Gauss Divergence Theorem for a vector function in the local $RT_{[0]}$ space.

Theorem 2 (Continuity of bulk normal flux). Let γ be a face shared by two hexahedra E_1, E_2 and $\mathbf{n}_1, \mathbf{n}_2$ be their (maybe non-constant) outward unit normal vectors. There holds

$$\int_\gamma \mathbf{u}_h^{(1)}\cdot\mathbf{n}_1 + \int_\gamma \mathbf{u}_h^{(2)}\cdot\mathbf{n}_2 = 0. \tag{9}$$

Proof. In Equation (4), we take a test function $q = \{q^\circ, q^\partial\}$ such that $q^\partial = 1$ only on γ; $q^\partial = 0$ on all other faces; $q^\circ = 0$ in the interior of any hexahedron. Applying the definitions for projection $\mathbf{Q}_h$ and discrete weak gradient, and again the Divergence Theorem, we obtain

$$\begin{aligned}0 &= \int_{E_1}(\mathbf{K}\nabla_{w,d}p_h)\cdot\nabla_{w,d}q + \int_{E_2}(\mathbf{K}\nabla_{w,d}p_h)\cdot\nabla_{w,d}q\\ &= \int_{E_1}\mathbf{Q}_h(\mathbf{K}\nabla_{w,d}p_h)\cdot\nabla_{w,d}q + \int_{E_2}\mathbf{Q}_h(\mathbf{K}\nabla_{w,d}p_h)\cdot\nabla_{w,d}q\\ &= \int_{E_1}(-\mathbf{u}_h^{(1)})\cdot\nabla_{w,d}q + \int_{E_1}(-\mathbf{u}_h^{(2)})\cdot\nabla_{w,d}q\\ &= -\int_\gamma q^\partial\mathbf{u}_h^{(1)}\cdot\mathbf{n}_1 + \int_{E_1} q^\circ\mathbf{u}_h^{(1)} - \int_\gamma q^\partial\mathbf{u}_h^{(2)}\cdot\mathbf{n}_2 + \int_{E_2} q^\circ\mathbf{u}_h^{(2)} = -\int_\gamma \mathbf{u}_h^{(1)}\cdot\mathbf{n}_1 - \int_\gamma \mathbf{u}_h^{(2)}\cdot\mathbf{n}_2.\end{aligned}$$

Theorem 3 (First order convergence in pressure, velocity, and flux). Assume the solution of the Darcy equation (3) has regularity $p\in H^2(\Omega), \mathbf{u}\in H^1(\Omega)$. Suppose the mesh is asymptotically parallelopiped. Then there holds

$$\|p - p_h^\circ\| \le Ch, \quad \|\mathbf{u}-\mathbf{u}_h\| \le Ch, \quad \|\mathbf{u}\cdot\mathbf{n} - \mathbf{u}_h\cdot\mathbf{n}\| \le Ch, \tag{10}$$

with the above norms defined respectively as

$$\|p - p_h^\circ\|^2 := \sum_{E\in\mathcal{E}_h} \|p - p_h^\circ\|^2_{L^2(E)}, \qquad \|\mathbf{u} - \mathbf{u}_h\|^2 := \sum_{E\in\mathcal{E}_h} \|\mathbf{u} - \mathbf{u}_h\|^2_{L^2(E)^3}, \tag{11}$$

$$\|(\mathbf{u} - \mathbf{u}_h)\cdot\mathbf{n}\|^2 := \sum_{E\in\mathcal{E}_h}\sum_{\gamma\subset E^\partial} \frac{|E|}{|\gamma|}\|\mathbf{u}\cdot\mathbf{n} - \mathbf{u}_h\cdot\mathbf{n}\|^2_{L^2(\gamma)}, \tag{12}$$

where C is a constant independent of the mesh size h, $|E|$ is the hexahedral volume, and $|\gamma|$ is the area of any face of the hexahedral element.

These theoretical results are similar to those presented in [6] for quadrilateral meshes. Further rigorous analysis will be presented in our future work.

4 Numerical Results

In this section, we present numerical experiments on three examples on two types of meshes. Type I meshes are logically 3-dim-rectangular. They are actually obtained from h^2-perturbations of uniform brick meshes on the unit cube, as used in [12]:

$$\begin{cases} x = \hat{x} + 0.03\sin(3\pi\hat{x})\cos(3\pi\hat{y})\cos(3\pi\hat{z}), \\ y = \hat{y} - 0.04\cos(3\pi\hat{x})\sin(3\pi\hat{y})\cos(3\pi\hat{z}), \\ z = \hat{z} + 0.05\sin(3\pi\hat{x})\cos(3\pi\hat{y})\sin(3\pi\hat{z}). \end{cases}$$

A Type II mesh starts from refinement of a tetrahedral mesh using the previously discussed THex algorithm and goes through regular refinement of hexahedral meshes. The mesh quality may not be good initially but improves with the successive refinement. The meshes satisfy the asymptotically parallelopiped assumption.

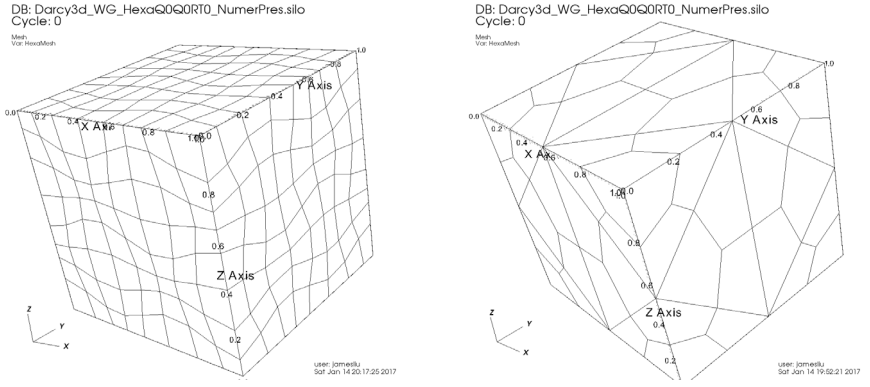

Type I mesh Type II mesh

Figure 2: Two types of hexahedral meshes. Type I: Logically rectangular and h^2-perturbed [12]; Type II: Applying the THex algorithm to a tetrahedral mesh and then successive refinements of hexahedral meshes.

Example 1. Here $\Omega = (0,1)^3$ (the unit cube), $\mathbf{K} = \mathbf{I}_3$, the exact pressure solution is $p(x,y,z) = \cos(\pi x)\cos(\pi y)\cos(\pi z)$. A Dirichlet boundary condition is specified on $\Gamma^D = \partial\Omega$ using the exact solution value. Shown in Figure 3 are the numerical pressure profiles for Type

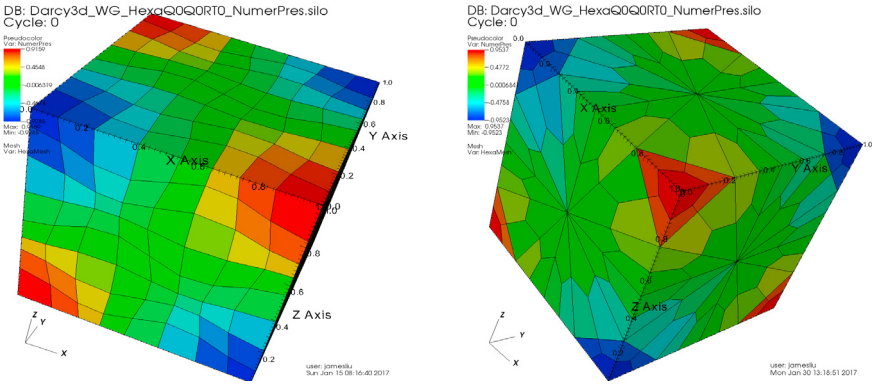

Type I mesh, $h = 1/8$ Type II mesh, $h = 1/8$

Figure 3: Example 1: Numerical pressure profiles on Type I and II hexahedral meshes.

I and II hexahedral meshes (both have mesh size $h = 1/8$. Shown in Table 1 are the numerical results from the WG $(Q_0, Q_0; RT_{[0]})$ finite element method. It is clearly observed that errors in pressure, velocity, and flux exhibit close to 1st order convergence.

Table 1: Example 1: Convergence of errors in pressure, velocity, and flux on Type I meshes

1/h	$\|p - p_h^\circ\|$	$\|\mathbf{u} - \mathbf{u}_h\|$	$\|(\mathbf{u} - \mathbf{u}_h) \cdot \mathbf{n}\|$
8	7.0011E-2	3.2844E-1	7.1386E-2
16	3.5623E-2	1.6527E-1	3.5469E-2
32	1.7905E-2	8.2288E-2	1.7623E-2
64	8.9652E-3	4.1069E-2	8.7969E-3
Conv.rate	0.988	0.999	1.006

Table 2: Example 2: Convergence of errors in pressure, velocity, and flux on Type I meshes

$1/h$	$\|p - p_h^\circ\|$	$\|\mathbf{u} - \mathbf{u}_h\|$	$\|(\mathbf{u} - \mathbf{u}_h) \cdot \mathbf{n}\|$
4	3.0310E-5	1.2359E-3	2.2008E-4
8	1.4466E-5	5.7003E-4	1.2107E-4
16	7.1904E-6	2.8141E-4	6.2760E-5
32	3.6280E-6	1.4303E-4	3.2173E-5
64	1.8858E-6	7.7512E-5	1.7172E-5
Conv.rate	1.001	0.998	0.920

Example 2. We have again $\Omega = (0,1)^3$, but a varying permeability and a known analytical solution for pressure provided as [12]

$$\mathbf{K} = \begin{bmatrix} y^2+2 & \cos(xy) & \sin(xz) \\ \cos(xy) & (x+3)^2 & \cos(yz) \\ \sin(xz) & \cos(yz) & (x+1)^2+z^2 \end{bmatrix}, \qquad p(x,y,z) = x^2(1-x)^2y^2(1-y)^2z^2(1-z)^2.$$

As seen in Table 2, for Type I hexahedral meshes, we have close to 1st order convergence in pressure, velocity, and flux.

Example 3 (Hexahedral meshes related to cylindrical coordinates). This example considers a cylindrical sector domain described as

$$\Omega = \{(r, \theta, z) : r_i \leq r \leq r_o, \alpha \leq \theta \leq \beta, z_b \leq z \leq z_t\}.$$

Assume the permeability in the three directions have values K_r, K_θ, K_z respectively and there is no any cross-wind permeability. Similar to [6], we can derive a permeability matrix in the Cartesian coordinates as

$$\mathbf{K}(x, y, z) = \begin{bmatrix} \frac{K_r x^2 + K_\theta y^2}{x^2+y^2} & \frac{(K_r - K_\theta)xy}{x^2+y^2} & 0 \\ \frac{(K_r - K_\theta)xy}{x^2+y^2} & \frac{K_r y^2 + K_\theta x^2}{x^2+y^2} & 0 \\ 0 & 0 & K_z \end{bmatrix}.$$

For numerical tests, we set $r_i = 1, r_o = 2, \alpha = 0, \beta = \frac{\pi}{2}, z_b = 0, z_t = 1$. We set $K_r = 10^{-1}, K_\theta = 10^{-3}, K_z = 1$ to examine anisotropy. We specify the exact pressure solution as $p(r, \theta, z) = r^2 \cos(\theta) \sin(\theta)(z^2 - z + 1)$. The source term in the Darcy equation is derived accordingly. A Dirichlet boundary condition is specified on the entire boundary of the domain using the pressure solution value.

Table 3: Example 3: Convergence of errors in pressure, velocity, and flux on hexahedral meshes for a cylindrical sector domain with uniform partitions in r, θ, z-directions

$n_r = n_\theta = n_z$	$\|p - p_h^\circ\|$	$\|\mathbf{u} - \mathbf{u}_h\|$	$\|(\mathbf{u} - \mathbf{u}_h) \cdot \mathbf{n}\|$
4	2.8496E-1	1.9865E-1	5.1197E-2
8	1.4716E-1	1.0206E-1	2.5189E-2
16	7.4176E-2	5.1302E-2	1.2528E-2
32	3.7162E-2	2.5668E-2	6.2531E-3
Conv.rate	0.979	0.984	1.011

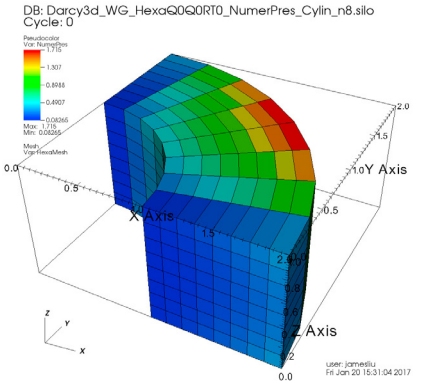

For partitions $n_r = n_\theta = n_z = 8$ (with mesh)

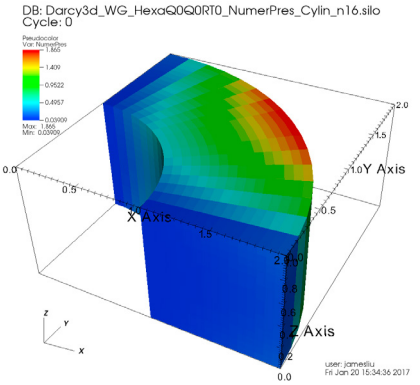

For partitions $n_r = n_\theta = n_z = 16$ (without mesh)

Figure 4: Example 3: Numerical pressure profiles on hexahedral meshes.

Applying uniform partitions in the r, θ, z-directions respectively with n_r, n_θ, n_z partitions, we obtain a hexahedral mesh. The hexahedra actually have flat faces. For simplicity, we use the

same number of partitions in the r, θ, z-directions. Shown in Table 3 are the numerical results of applying the WG$(Q_0, Q_0; RT_{[0]})$ finite element method. Close to 1st order convergence rates in pressure, velocity, and flux are observed. Shown in Figure 4 are the numerical pressure profiles for respectively $n_r = n_\theta = n_z = 8$ and $n_r = n_\theta = n_z = 16$.

5 Concluding Remarks

As investigated in this paper, the THex algorithm can be employed to refine a tetrahedral mesh into a hexahedral mesh. Then finite element solvers on these two types of meshes can be compared for DOFs, accuracy, and other solution properties. The hexahedral meshes generated this way usually involve obtuse dihedral angles and the mesh quality is not high. Among free and commercial mesh generators, `Gmsh`, `CUBIT/Trelis` can be used to generate hexahedral meshes with better quality.

The weak Galerkin finite elements $(Q_0, Q_0; RT_{[0]})$ have be used to solve the Darcy equation on hexahedral meshes. This Darcy solver is easier in implementation, compared to those solvers using the mixed finite elements based on the Piola transformation [2] or the WG solvers involving stabilizers [7]. This simple solver is locally mass-conservative and produces continuous normal fluxes, regardless of hexahedral mesh quality. It exhibits optimal convergence in pressure, velocity, and flux when the hexahedral mesh is asymptotically parallelopiped. Therefore, it is a practically useful Darcy solver.

References

[1] Csimsoft. *Trelis: Advanced meshing for challenging simulations.*

[2] R. Falk, P. Gatto, and P. Monk. Hexahedral $h(div)$ and $h(curl)$ finite elements. *M2AN*, 45:115–143, 2011.

[3] B. Ganis, M. F. Wheeler, and I. Yotov. An enhanced velocity multipoint flux mixed finite element method for darcy flow on non-matching hexahedral grids. *Proc. Comput. Sci.*, 51:1198–1207, 2015.

[4] G. Lin, J. Liu, L. Mu, and X. Ye. Weak galerkin finite element methdos for darcy flow: Anistropy and heterogeneity. *J. Comput. Phys.*, 276:422–437, 2014.

[5] G. Lin, J. Liu, and F. Sadre-Marandi. A comparative study on the weak galerkin, discontinuous galerkin, and mixed finite element methods. *J. Comput. Appl. Math.*, 273:346–362, 2015.

[6] J. Liu, S. Tavener, and Z. Wang. The lowest-order weak galerkin finite element methods for the darcy equation on quadrilateral and hybrid meshes. *J. Comput. Phys.*, 0:Manuscript submitted, 2017.

[7] L. Mu, J. Wang, and X. Ye. A weak galerkin finite element method with polynomial reduction. *J. Comput. Appl. Math.*, 285:45–58, 2015.

[8] J. Remacle, J. Lambrechts, B. Seny, E. Marchandise, A. Johnen, and C. Geuzainet. Blossom-quad: A non-uniform quadrilateral mesh generator using a minimum-cost perfect-matching algorithm. *Int. J. Numer. Meth. Engrg.*, 89:1102–1119, 2012.

[9] H. Shi. *TetGen: A quality tetrahedral mesh generator and a 3d Delaunay triangulator.*

[10] S. Sun and J. Liu. A locally conservative finite element method based on piecewise constant enrichment of the continuous galerkin method. *SIAM J. Sci. Comput.*, 31:2528–2548, 2009.

[11] J. Wang and X. Ye. A weak galerkin finite element method for second order elliptic problems. *J. Comput. Appl. Math.*, 241:103–115, 2013.

[12] M. Wheeler, G. Xue, and I. Yotov. A multipoint flux mixed finite element method on distorted quadrilaterals and hexahedra. *Numer. Math.*, 121:165–204, 2012.